

Small, narrowly distributed iridium nanoparticles supported on indium tin oxide for efficient anodic water oxidation

Journal Article

Author(s):

[Lebedev, Dmitry](#) ; [Copéret, Christophe](#) 

Publication date:

2019-01

Permanent link:

<https://doi.org/10.3929/ethz-b-000342525>

Rights / license:

[In Copyright - Non-Commercial Use Permitted](#)

Originally published in:

ACS Applied Energy Materials 2(1), <https://doi.org/10.1021/acsaem.8b01724>

Small, Narrowly Distributed Iridium Nanoparticles Supported on Indium Tin Oxide for Efficient Anodic Water Oxidation

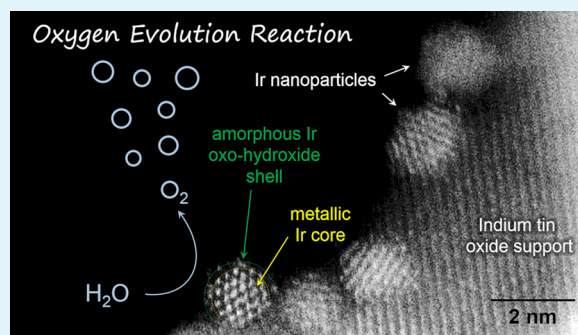
Dmitry Lebedev¹ and Christophe Copéret^{1*}

Department of Chemistry and Applied Biosciences, ETH Zurich, Vladimir Prelog Weg 1–5, CH–8093 Zurich, Switzerland

Supporting Information

ABSTRACT: Decreasing the noble metal content while maintaining high catalytic activity is a critical requirement for the development of efficient anodic water oxidation catalysts in acidic media. In the present work, we developed a method for immobilizing 1.5 nm Ir nanoparticles on a conductive indium tin oxide support. In addition to having a low Ir content of 4.1 wt %, the obtained Ir_{NP}-ITO material is very active and stable in water oxidation, reaching a current of 10 A g_{Ir}⁻¹ at 1.470 V vs RHE. Our electrode design allows for convenient analysis of the catalyst after the electrochemical tests. Employing high resolution electron microscopy, we show that under the OER conditions, the core of iridium particles stays metallic, while amorphous layer forms on the particle surface, which we attribute to Ir-oxo-hydroxide based on our X-ray photoelectron spectroscopy studies. The surface Ir-oxo-hydroxide layer is responsible for the high OER efficiency of the supported catalyst.

KEYWORDS: oxygen evolution reaction, water oxidation, indium tin oxide, iridium nanoparticles, electrocatalysis



Hydrogen is an attractive alternative to fossil fuels that allows for sustainable energy supply without contributing to global warming or CO₂ emission.¹ Renewable generation of hydrogen can be achieved via water splitting, which can be either driven by solar energy (artificial photosynthesis)² or electricity (water electrolysis).^{3,4} Water electrolysis is typically performed under either basic (alkali water electrolysis) or acidic (polymer electrolyte membrane water electrolysis) conditions with the latter having a number of advantages, including the possibility to achieve higher pressures of H₂ and maintaining high-voltage efficiencies at high current densities.³ Another advantage of acidic water electrolysis is the high efficiency of the cathodic hydrogen generation (hydrogen evolution reaction, HER) catalyzed by platinum. On the other hand, the concomitant anodic process (oxygen evolution reaction, OER) suffers from high overpotentials and sluggish kinetics, therefore limiting the overall performance of electrolyzer.^{5–7} Moreover, harsh OER conditions in acidic media limit the pool of possible catalysts to noble metals (Ru and Ir), which are highly expensive and scarce.⁸ Thus, lowering the noble metal content becomes an essential requirement for the practical implementation of acidic water electrolyzers.⁹

Decreasing the noble metal loading can be achieved via synthesis of high surface area noble metal oxides^{10,11} or by combining noble metals with other conductive materials to make hybrid catalysts, where nanosized blocks of noble metals are embedded in the matrix of conductive support.¹² While carbon-based supports are often used (because of their high surface area, high conductivity, and low weight), their major

disadvantage is the degradation under harsh OER conditions.¹³ As an alternative to carbon, conductive oxide-based supports are proposed, including doped titanium, tin, or indium oxides.^{14–17} Moreover, recent studies show that the presence of the metal/metal oxide support interactions can lead to improvement of the catalyst stability under OER conditions.¹⁸

Previous efforts of preparing hybrid catalysts mostly focused on either reduction or hydrolysis of the noble metal precursors (often IrCl₃) in the presence of the conductive oxide¹⁸ or by simultaneous formation of both oxides (e.g., using sol-gel or Adams fusion method).^{14,19} These approaches often lead to the ill-defined architecture of the hybrid material, which complicates the detailed structural studies, e.g. via high resolution electron microscopy.

Here, we develop a convenient and robust method for generating small and narrowly distributed 1.5 ± 0.2 nm Ir nanoparticles immobilized on an ITO support, Ir_{NP}-ITO. Ir_{NP}-ITO is a very efficient electrocatalyst that displays high OER activity and stability while having low Ir content. High resolution electron microscopy in combination with X-ray photoelectron spectroscopy (XPS) studies reveal that the Ir nanoparticles evolve under OER conditions to generate core-shell structure, where the core remains metallic while the outer layer oxidizes to amorphous Ir-oxo-hydroxide.

Colloidal Ir nanoparticles were prepared via a solvothermal method²⁰ and deposited on porous ITO films fabricated on

Received: October 9, 2018

Accepted: December 13, 2018

Published: December 13, 2018

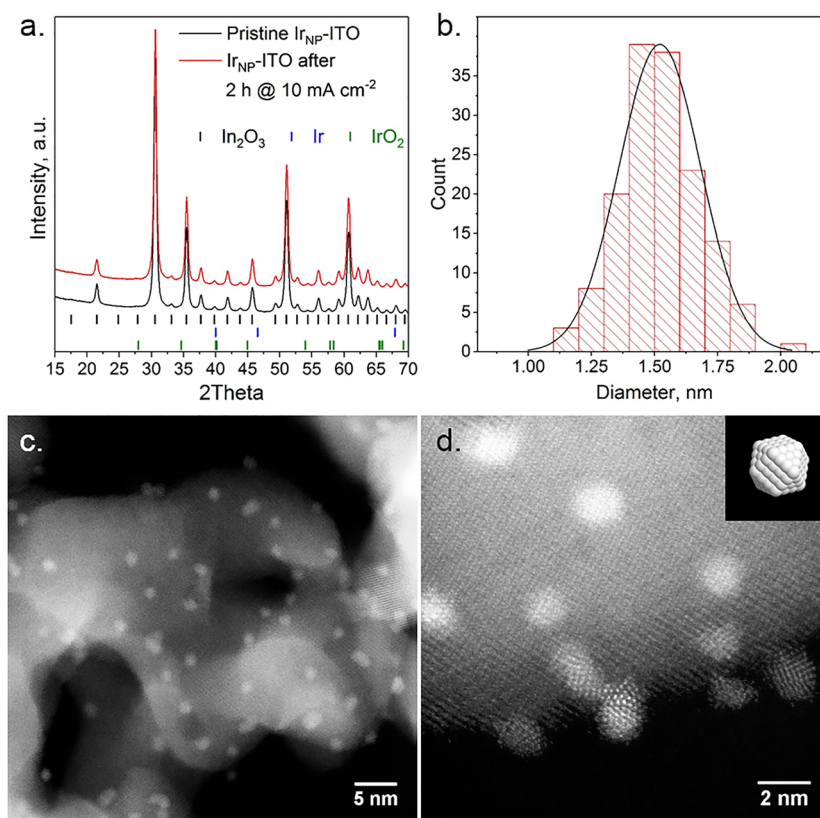


Figure 1. (a) Powder XRD of Ir_{NP}-ITO before (pristine, black) and after 2 h at 10 mA cm⁻² (red). No peaks of Ir or IrO₂ are observed. (b) Ir particle size distribution with the mean diameter of 1.5 ± 0.2 nm. (c, d) HAADF-STEM images of the pristine Ir_{NP}-ITO. Inset: 1.5 nm Ir particle of cuboctahedron shape.

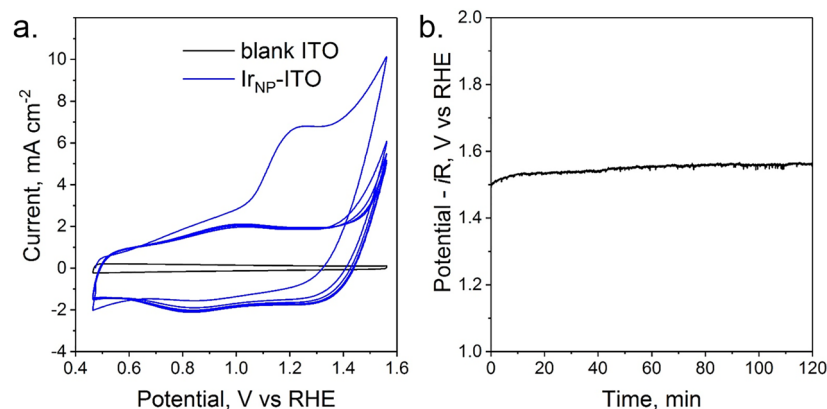


Figure 2. (a) Cyclic voltammetry of blank ITO (black) and Ir_{NP}-ITO (blue), 0.1 M HClO₄, 25 mV s⁻¹. 1st, 5th, 10th, 15th, and 20th cycles are shown. (b) Chronopotentiometry of Ir_{NP}-ITO: 2 h at 10 mA cm⁻².

fluorine-doped tin oxide (FTO) glass substrates,^{21,22} yielding Ir_{NP}-ITO (see the [Supporting Information](#) for the detailed procedures). Powder X-ray diffraction (XRD) studies of Ir_{NP}-ITO ([Figure 1a](#)) show exclusively peaks of indium oxide with no signals corresponding to iridium or iridium dioxide, which indicates the absence of large Ir-containing crystallites. High-angle annular dark field scanning transmission electron microscopy (HAADF-STEM) shows a homogeneous distribution of spherical and highly crystalline iridium particles on the ITO support with an average diameter of 1.5 ± 0.2 nm ([Figures 1b–d](#) and [Figure S1 of the Supporting Information](#)). High-resolution images ([Figure S2 of the Supporting Information](#)) confirm the formation of a metallic Ir structure.

Crystalline Ir nanoparticle with the size of 1.5 nm has approximately 150 atoms with 90 Ir atoms being on the surface (see inset on the [Figure 1d](#)), which allows for the efficient utilization of the noble metal in the catalyst (up to 60%).

Elemental analysis of the Ir_{NP}-ITO electrodes gives an iridium loading of 4.1 wt %, corresponding to a density of 530 ± 30 nmol(Ir) cm⁻² (102 μg(Ir) cm⁻², see [Supporting Information](#) for details), which is significantly lower compared to previous reports of supported IrO₂ nanoparticles.^{14,16,18,23}

Electrochemical studies of Ir_{NP}-ITO were performed in 0.1 M HClO₄ electrolyte (see details in the [Supporting Information](#)). The first scan in the anodic direction in cyclic voltammetry studies ([Figure 2a](#)) shows an irreversible peak at

approximately 1.2 V vs RHE, which can be attributed to the removal of the PVP ligand and oxidation of the nanoparticle surface, with the core of the particle remaining metallic (*vide infra*).¹⁵ Subsequent cycling reveals a reversible redox wave at 0.94 V vs RHE (attributed to the Ir^{IV/III} couple, see Figures S3 and S5 of the Supporting Information) followed by a current increase (onset of OER).

The OER catalytic activity of Ir_{NP}-ITO was examined using chronoamperometric measurements. The Tafel plot of Ir_{NP}-ITO (Figure S4 of the Supporting Information) has a slope of 52 ± 5 mV dec⁻¹, which is similar to the previous reports on Ir nanodendrites (56 – 58 mV dec⁻¹),¹⁵ unsupported Ir nanoparticles (51.4 mV dec⁻¹),²⁴ and antimony tin oxide (ATO) supported Ir nanoparticles (57 – 60 mV dec⁻¹). Smaller Tafel slope of 40 mV dec⁻¹ was reported for high purity, unsupported Ir nanoparticles.²⁵ Ir_{NP}-ITO displays a current of 10 A g_{Ir}⁻¹ at 1.470 ± 0.005 V vs RHE, which is lower than that reported for high surface area IrO₂ and IrO₂-TiO₂ catalysts (1.485 – 1.497 V).^{10,14} At 1.48 V vs RHE, Ir_{NP}-ITO produces a current of 16 ± 3 A g_{Ir}⁻¹, similar to 24 A g_{Ir}⁻¹ reported for high purity Ir nanoparticles.²⁵ At a higher potential of 1.51 vs RHE, Ir_{NP}-ITO produces a current of 35 ± 3 A g_{Ir}⁻¹, which is similar to approximately 40 A g_{Ir}⁻¹ reported for ATO supported Ir nanoparticles,¹⁸ yet lower than that reported for the state-of-the-art metallic Ir catalysts (70 A g_{Ir}⁻¹ for Ir nanodendrites¹⁵ and 100 A g_{Ir}⁻¹ for high purity Ir nanoparticles²⁵). The slightly lower activity obtained at high potentials can be attributed to the fact that 1.5 cm² flat electrodes are used here in contrast to the approximately 0.2 cm² rotating disk electrodes commonly used for OER activity evaluation. Large electrode surfaces (hence high absolute current) and an inability to rotate the electrode cause problems with diffusion and oxygen bubble removal at high potentials. On the other hand, the advantages of flat electrodes are the possibility to couple the electrochemical measurements with the spectroscopy (X-ray, UV-vis-IR)²² and to perform analysis of the OER catalysts postelectrolysis. The latter is due to the larger amount of catalyst on the electrode surface and absence of binders often used for the rotating disk electrode studies (carbon black, Nafion, etc.).

To test the stability of Ir_{NP}-ITO, 2-h electrolysis tests at 10 mA cm⁻² were performed.⁸ A flat potential profile was obtained during the course of the measurement (Figure 2b), indicating good OER stability. On average, the Ir_{NP}-ITO catalyst requires an overpotential of 340 ± 20 mV to drive the current of 10 mA cm⁻².

As mentioned above, the use of flat electrodes with high catalyst loading allows for postelectrolysis analysis of the catalyst. Similar to the pristine electrodes, the powder XRD pattern of Ir_{NP}-ITO after a 2-h stability test at 10 mA cm⁻² shows exclusively peaks of iridium oxide, indicating the absence of large Ir containing crystallites (Figure 1a). We further performed the HAADF-STEM imaging of the Ir_{NP}-ITO after 20 CV cycles from 0.5 to 1.35 V vs RHE (Figures S5 and S6 of the Supporting Information) and after 2-h stability test at 10 mA cm⁻² (Figure 3 and Figures S7 and S8 of the Supporting Information). Both samples show a slight increase of the iridium nanoparticle size from 1.5 ± 0.2 to 1.6 ± 0.2 nm and 1.7 ± 0.2 nm, respectively. High resolution images (Figure 3c and Figures S6 and S8 of the Supporting Information) clearly show that the core of Ir particles remains metallic. This observation is in line with the ATO supported Ir nanoparticles¹⁸ and the recent report on the high purity Ir

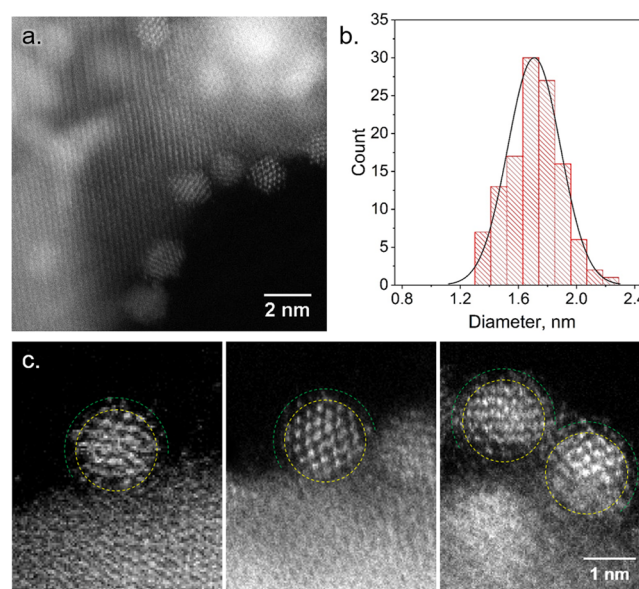


Figure 3. (a) HAADF-STEM image, (b) particle size distribution, and (c) high resolution HAADF-STEM images of Ir_{NP}-ITO after chronopotentiometric measurement (2-h electrolysis at 10 mA cm⁻²). The dotted lines indicate the oxidized Ir-oxo-hydroxide shell surrounding the metallic core.

nanoparticles, where *operando* near-ambient pressure XPS indirectly showed that the core of the Ir particles remains metallic under OER conditions.²⁵ In addition to the metallic core, high resolution images of Ir_{NP}-ITO after both CV cycling (20 CV cycles from 0.5 to 1.35 V vs RHE, Figure S6 of the Supporting Information) and OER (2 h at 10 mA cm⁻², Figure 3c) indicate the presence of an amorphous surface layer, which we attribute to the iridium oxo-hydroxide shell formed upon electrochemical oxidation (*vide infra*). The layer formation likely accounts for the slight increase of the nanoparticle size. However, one should note that the electrochemically oxidized surface layer might be modified under TEM imaging conditions (partially reduced by electrons); hence, the layer thickness estimation or other detailed analyses should be taken with care. The iridium oxo-hydroxide layer was previously proposed for Ir nanoparticles supported on ATO,¹⁸ IrO₂/Ir particles,²⁶ iridium oxide,¹⁰ and complex iridium oxides;^{27,28} however, to the best of our knowledge, the layer has never been observed using microscopy studies. Formation of the oxo-hydroxide layer was previously associated with the high OER activity and stability.^{10,18}

To understand the electronic state of iridium in the Ir_{NP}-ITO catalyst before and after the stability test, we carried out XPS studies (see the Supporting Information for details and Figure S9). The Ir 4f region (Figure 4) consists of two asymmetric peaks which are assigned to spin-orbit split Ir 4f components: Ir 4f 7/2 and Ir 4f 5/2. The spectra were fit using an asymmetrical Lorentzian line-shape, resulting in the energy of 60.4 eV (Ir 4f 7/2) for the pristine Ir_{NP}-ITO, which corresponds to metallic Ir. After the 2-h electrolysis test at 10 mA cm⁻², Ir 4f 7/2 energy is shifted by 0.7 eV (61.1 eV), indicating oxidation of iridium. Because the Ir 4f 7/2 energy of IrO₂ is reported to be in the range of 61.7–62.5 eV,^{10,29,30} the energy of 61.1 eV corresponds to the mixture of metallic and oxidized Ir. Therefore, taking into account the small size of

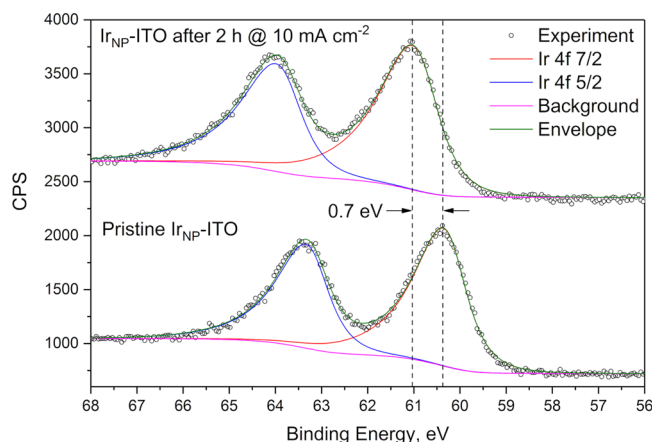


Figure 4. XPS studies of Ir_{NP}-ITO before (pristine) and after 2 h at 10 mA cm⁻². Fitting of the experimental data was performed using asymmetrical Lorentzian line shape.

iridium nanoparticles, the XPS data together with the high resolution electron microscopy show that the core of the particle stays metallic while the particle surface gets oxidized to the form of iridium oxo-hydroxide layer. Formation of this amorphous layer (Figure 3c) causes the slight increase of the nanoparticle size revealed by the electron microscopy studies.

In conclusion, we report a robust method for the preparation of highly active and stable electrodes for anodic water oxidation in acidic media. Owing to the small size of the Ir nanoparticles, most iridium atoms are located on the particle surface, allowing for the efficient iridium utilization. High resolution microscopy data allowed for the direct observation of an amorphous surface layer (with the particle core being metallic), which is attributed to Ir-oxo-hydroxide based on complementary XPS data. The Ir-oxo-hydroxide layer, formed upon electrochemical oxidation of the Ir particle surface, is responsible for the high activity of the catalyst. We anticipate that the proposed approach of nanoparticle immobilization on porous ITO electrodes is suitable for studying electrochemical properties of a broad range of metallic and oxide particles (e.g., Ir-Ru, Ir-Ni, etc.) in combination with advanced spectroscopy and high resolution microscopy tools. Moreover, due to the unique properties of ITO, the proposed approach is suitable for preparation of transparent electrodes which can be used in solar-driven water splitting devices. We are currently exploring these directions.

■ ASSOCIATED CONTENT

Supporting Information

The Supporting Information is available free of charge on the ACS Publications website at DOI: 10.1021/acsam.8b01724.

Materials, methods, and detailed procedures; additional HAADF-STEM, XPS, and electrochemical data (PDF)

■ AUTHOR INFORMATION

Corresponding Author

*E-mail: ccoperet@ethz.ch

ORCID

Dmitry Lebedev: 0000-0002-1866-9234

Christophe Copéret: 0000-0001-9660-3890

Funding

The authors would like to acknowledge the Competence Center Energy and Mobility (CCEM-CH, Project Renerg2), the Commission for Technology and Innovation Switzerland, and the Swiss Competence Center for Energy Research (SCCER) Heat and Electricity Storage as well as the Swiss Federal Office of Energy and Swiss Electric Research for their financial support. The authors also would like to thank the Swiss National Foundation (project 206021_164012) for their support with the JEOL JEM-ARM 200CF transmission electron microscope.

Notes

The authors declare no competing financial interest.

■ ACKNOWLEDGMENTS

The authors would like to acknowledge Dr. Xing Huang (Scientific center for optical and electron microscopy (ScopeM), ETH Zurich, Switzerland) for performing the electron microscopy measurements and Dr. Juan Herranz (Paul Scherrer Institute, Villigen, Switzerland) for performing the XPS measurements.

■ REFERENCES

- (1) Rau, G. H.; Willauer, H. D.; Ren, Z. J. The global potential for converting renewable electricity to negative-CO₂-emissions hydrogen. *Nat. Clim. Change* **2018**, *8*, 621–625.
- (2) Tachibana, Y.; Vayssieres, L.; Durrant, J. R. Artificial photosynthesis for solar water-splitting. *Nat. Photonics* **2012**, *6*, 511–518.
- (3) Ursua, A.; Gandia, L. M.; Sanchis, P. Hydrogen Production From Water Electrolysis: Current Status and Future Trends. *Proc. IEEE* **2012**, *100*, 410–426.
- (4) Seh, Z. W.; Kibsgaard, J.; Dickens, C. F.; Chorkendorff, I.; Nørskov, J. K.; Jaramillo, T. F. Combining theory and experiment in electrocatalysis: Insights into materials design. *Science* **2017**, *355*, No. eaad4998.
- (5) Suen, N. T.; Hung, S. F.; Quan, Q.; Zhang, N.; Xu, Y. J.; Chen, H. M. Electrocatalysis for the oxygen evolution reaction: recent development and future perspectives. *Chem. Soc. Rev.* **2017**, *46*, 337–365.
- (6) Spori, C.; Kwan, J. T. H.; Bonakdarpour, A.; Wilkinson, D. P.; Strasser, P. The Stability Challenges of Oxygen Evolving Catalysts: Towards a Common Fundamental Understanding and Mitigation of Catalyst Degradation. *Angew. Chem., Int. Ed.* **2017**, *56*, 5994–6021.
- (7) Reier, T.; Nong, H. N.; Teschner, D.; Schlögl, R.; Strasser, P. Electrocatalytic Oxygen Evolution Reaction in Acidic Environments - Reaction Mechanisms and Catalysts. *Adv. Energy Mater.* **2017**, *7*, 1601275.
- (8) McCrory, C. C.; Jung, S.; Peters, J. C.; Jaramillo, T. F. Benchmarking heterogeneous electrocatalysts for the oxygen evolution reaction. *J. Am. Chem. Soc.* **2013**, *135*, 16977–16987.
- (9) Babic, U.; Suermann, M.; Gubler, L.; Büchi, F. N.; Schmidt, T. J. Identifying critical gaps for polymer electrolyte water electrolysis development. *J. Electrochem. Soc.* **2017**, *164*, F1–F13.
- (10) Abbott, D. F.; Lebedev, D.; Waltar, K.; Povia, M.; Nachttegaal, M.; Fabbri, E.; Copéret, C.; Schmidt, T. J. Iridium Oxide for the Oxygen Evolution Reaction: Correlation between Particle Size, Morphology, and the Surface Hydroxide Layer from Operando XAS. *Chem. Mater.* **2016**, *28*, 6591–6604.
- (11) Li, G.; Li, S.; Xiao, M.; Ge, J.; Liu, C.; Xing, W. Nanoporous IrO₂ catalyst with enhanced activity and durability for water oxidation owing to its micro/mesoporous structure. *Nanoscale* **2017**, *9*, 9291–9298.
- (12) Shao, Y.; Liu, J.; Wang, Y.; Lin, Y. Novel catalyst support materials for PEM fuel cells: current status and future prospects. *J. Mater. Chem.* **2009**, *19*, 46–59.

- (13) Wang, J.; Yin, G.; Shao, Y.; Zhang, S.; Wang, Z.; Gao, Y. Effect of carbon black support corrosion on the durability of Pt/C catalyst. *J. Power Sources* **2007**, *171*, 331–339.
- (14) Oakton, E.; Lebedev, D.; Povia, M.; Abbott, D. F.; Fabbri, E.; Fedorov, A.; Nachtegaal, M.; Copéret, C.; Schmidt, T. J. IrO₂-TiO₂: A High-Surface-Area, Active, and Stable Electrocatalyst for the Oxygen Evolution Reaction. *ACS Catal.* **2017**, *7*, 2346–2352.
- (15) Oh, H.-S.; Nong, H. N.; Reier, T.; Gliech, M.; Strasser, P. Oxide-supported Ir nanodendrites with high activity and durability for the oxygen evolution reaction in acid PEM water electrolyzers. *Chem. Sci.* **2015**, *6*, 3321–3328.
- (16) Puthiyapura, V. K.; Pasupathi, S.; Su, H.; Liu, X.; Pollet, B.; Scott, K. Investigation of supported IrO₂ as electrocatalyst for the oxygen evolution reaction in proton exchange membrane water electrolyser. *Int. J. Hydrogen Energy* **2014**, *39*, 1905–1913.
- (17) Wang, Y. J.; Wilkinson, D. P.; Zhang, J. Noncarbon support materials for polymer electrolyte membrane fuel cell electrocatalysts. *Chem. Rev.* **2011**, *111*, 7625–7651.
- (18) Oh, H.-S.; Nong, H. N.; Reier, T.; Bergmann, A.; Gliech, M.; Ferreira de Araújo, J.; Willinger, E.; Schlögl, R.; Teschner, D.; Strasser, P. Electrochemical Catalyst-Support Effects and Their Stabilizing Role for IrO_x Nanoparticle Catalysts during the Oxygen Evolution Reaction. *J. Am. Chem. Soc.* **2016**, *138*, 12552–12563.
- (19) Puthiyapura, V. K.; Pasupathi, S.; Basu, S.; Wu, X.; Su, H.; Varaganapandiyam, N.; Pollet, B.; Scott, K. RuxNb_{1-x}O₂ catalyst for the oxygen evolution reaction in proton exchange membrane water electrolyzers. *Int. J. Hydrogen Energy* **2013**, *38*, 8605–8616.
- (20) Zhang, T.; Li, S.-C.; Zhu, W.; Ke, J.; Yu, J.-W.; Zhang, Z.-P.; Dai, L.-X.; Gu, J.; Zhang, Y.-W. Iridium ultrasmall nanoparticles, worm-like chain nanowires, and porous nanodendrites: One-pot solvothermal synthesis and catalytic CO oxidation activity. *Surf. Sci.* **2016**, *648*, 319–327.
- (21) Farnum, B. H.; Morseth, Z. A.; Brennaman, M. K.; Papanikolas, J. M.; Meyer, T. J. Driving force dependent, photoinduced electron transfer at degenerately doped, optically transparent semiconductor nanoparticle interfaces. *J. Am. Chem. Soc.* **2014**, *136*, 15869–15872.
- (22) Lebedev, D.; Pineda-Galvan, Y.; Tokimaru, Y.; Fedorov, A.; Kaeffer, N.; Coperet, C.; Pushkar, Y. The Key Ru(V)=O Intermediate of Site-Isolated Mononuclear Water Oxidation Catalyst Detected by in Situ X-ray Absorption Spectroscopy. *J. Am. Chem. Soc.* **2018**, *140*, 451–458.
- (23) Oakton, E.; Lebedev, D.; Fedorov, A.; Krumeich, F.; Tillier, J.; Sereda, O.; Schmidt, T. J.; Copéret, C. A simple one-pot Adams method route to conductive high surface area IrO₂-TiO₂ materials. *New J. Chem.* **2016**, *40*, 1834–1838.
- (24) Fu, L.; Zeng, X.; Huang, C.; Cai, P.; Cheng, G.; Luo, W. Ultrasmall Ir nanoparticles for efficient acidic electrochemical water splitting. *Inorg. Chem. Front.* **2018**, *5*, 1121–1125.
- (25) Lettenmeier, P.; Majchel, J.; Wang, L.; Saveleva, V. A.; Zafeiratos, S.; Savinova, E. R.; Gallet, J. J.; Bournel, F.; Gago, A. S.; Friedrich, K. A. Highly active nano-sized iridium catalysts: synthesis and operando spectroscopy in a proton exchange membrane electrolyzer. *Chem. Sci.* **2018**, *9*, 3570–3579.
- (26) Minguzzi, A.; Locatelli, C.; Lugaresi, O.; Achilli, E.; Cappelletti, G.; Scavini, M.; Coduri, M.; Masala, P.; Sacchi, B.; Vertova, A.; Ghigna, P.; Rondinini, S. Easy Accommodation of Different Oxidation States in Iridium Oxide Nanoparticles with Different Hydration Degree as Water Oxidation Electrocatalysts. *ACS Catal.* **2015**, *5*, 5104–5115.
- (27) Lebedev, D.; Povia, M.; Waltar, K.; Abdala, P. M.; Castelli, I. E.; Fabbri, E.; Blanco, M. V.; Fedorov, A.; Copéret, C.; Marzari, N.; Schmidt, T. J. Highly Active and Stable Iridium Pyrochlores for Oxygen Evolution Reaction. *Chem. Mater.* **2017**, *29*, 5182–5191.
- (28) Seitz, L. C.; Dickens, C. F.; Nishio, K.; Hikita, Y.; Montoya, J.; Doyle, A.; Kirk, C.; Vojvodic, A.; Hwang, H. Y.; Norskov, J. K.; Jaramillo, T. F. A highly active and stable IrO_x/SrIrO₃ catalyst for the oxygen evolution reaction. *Science* **2016**, *353*, 1011–1014.
- (29) Freakley, S. J.; Ruiz-Esquius, J.; Morgan, D. J. The X-ray photoelectron spectra of Ir, IrO₂ and IrCl₃ revisited. *Surf. Interface Anal.* **2017**, *49*, 794–799.
- (30) Pfeifer, V.; Jones, T. E.; Velasco Vélez, J. J.; Massué, C.; Arrigo, R.; Teschner, D.; Girgsdies, F.; Scherzer, M.; Greiner, M. T.; Allan, J.; Hashagen, M.; Weinberg, G.; Piccinin, S.; Hävecker, M.; Knop-Gericke, A.; Schlögl, R. The electronic structure of iridium and its oxides. *Surf. Interface Anal.* **2016**, *48*, 261–273.